

# RRATs: New Discoveries, Timing Solutions & Musings

E.F. Keane<sup>1</sup>, M. Kramer<sup>1,2</sup>, A.G. Lyne<sup>1</sup>, B.W. Stappers<sup>1</sup> & M.A. McLaughlin<sup>3,4</sup>

<sup>1</sup> *University of Manchester, Jodrell Bank Centre for Astrophysics, School of Physics & Astronomy, Manchester M13 9PL, UK.*

<sup>2</sup> *Max Planck Institut für Radioastronomie, Auf dem Hügel 69, 53121 Bonn, Germany.*

<sup>3</sup> *Department of Physics, West Virginia University, Morgantown, WV 26506, USA .*

<sup>4</sup> *Also adjunct at the National Radio Astronomy Observatory, Green Bank, WV, USA.*

1 January 2011

## ABSTRACT

We describe observations of Rotating RADio Transients (RRATs) that were discovered in a re-analysis of the Parkes Multi-beam Pulsar Survey (PMPS). The sources have now been monitored for sufficiently long to obtain seven new coherent timing solutions, to make a total of 14 now known. Furthermore we announce the discovery of 7 new transient sources, one of which may be extragalactic in origin (with  $z \sim 0.1$ ) and would then be a second example of the so-called ‘Lorimer burst’. The timing solutions allow us to infer neutron star characteristics such as energy-loss rate, magnetic field strength and evolutionary timescales, as well as facilitating multi-wavelength followup by providing accurate astrometry. All of this enables us to consider the question of whether or not RRATs are in any way special, i.e. a distinct and separate population of neutron stars, as has been previously suggested. We see no reason to consider ‘RRAT’ as anything other than a detection label, the subject of a selection effect in the parameter space searched. However, single-pulse searches can be utilised to great effect to identify pulsars difficult, or impossible, to find by other means, in particular those with long-periods (half of the PMPS RRATs have periods greater than 4 seconds), high-magnetic field strengths ( $B \gtrsim 10^{13}$  G) and pulsars approaching the ‘death valley’. The detailed nulling properties of such pulsars are unknown but the mounting evidence suggests a broad range of behaviour in the pulsar population. The group of RRATs fit in to the picture where pulsar magnetospheres switch between stable configurations.

**Key words:** stars:neutron – pulsars: general – Galaxy: stellar content – ephemerides – surveys

## 1 INTRODUCTION

A recent highlight in radio transient searches has been the discovery of RRATs (Rotating RADio Transients) by McLaughlin et al. (2006) (M+06 from herein). RRATs have primarily been studied at radio frequencies of 1.4 GHz, where they exhibit detectable emission only sporadically, with millisecond-duration bursts every few minutes to hours. They are believed to be neutron stars, for a number of reasons: (1) Causality implies that pulses of width  $W$  originate from emission regions with size  $\leq 300 \text{ km}(W/1 \text{ ms})$ , which in the case of RRATs (pulse widths of  $\sim 1 - 30 \text{ ms}$ ) is much smaller than typical white dwarf radii. RRAT pulse widths are also similar to the single pulse widths of radio pulsars (see e.g. Lorimer & Kramer (2005)). Furthermore, the dynamical time  $t_{\text{dyn}} = 1/\sqrt{G\rho}$ , where  $G$  is Newton’s constant and  $\rho$  is mass density, is the scale on which we expect to see changes, so that the millisecond radio sky consists mainly of neutron stars which have  $t_{\text{dyn,NS}} \sim 0.1 \text{ ms}$ , whereas tran-

sient emission can be expected from white dwarfs on longer timescales of  $t_{\text{dyn,WD}} \sim 1 - 10 \text{ s}$ ; (2) Their pulses have high brightness temperatures of  $\sim 10^{20} - 10^{24} \text{ K}$ , similar to radio pulsars (see Figure 1); (3) Their underlying periodicities span the range  $0.1 - 7.7 \text{ s}$ , typical neutron star rotation periods; (4) One source, J1819–1458 has been observed in the X-ray, showing thermal emission at  $\sim 140 \text{ eV}$ , as expected for a cooling neutron star (Reynolds et al. 2006; McLaughlin et al. 2007; Rea et al. 2009); (5) In those sources which have been well studied, their periods are seen to increase at rates similar to those seen in other neutron star classes (McLaughlin et al. 2006, 2009).

It was initially thought that the RRATs may constitute a heretofore unknown, distinct population of Galactic neutron stars. However, this seems unlikely, as when the large projected population of RRATs is incorporated into the menagerie of other known neutron star classes, a problem results. If the known neutron star groups are distinct, then the Galactic supernova rate is insufficient to explain the

number of neutron stars which we infer (Keane & Kramer 2008). This problem can be removed if the groups of neutron stars are evolutionarily linked and/or if their projected populations are over-estimated. An evolutionary link between the various classes would, in some senses, be satisfactory, as such links must exist. However neutron star spin evolution is poorly understood, and no such evolutionary framework exists (see Vranešević & Melrose (2010) for a recent discussion of this). A large over-estimate of the population is also possible, given the large extrapolation from a small number of known objects to an entire Galactic population.

Such motives resulted in our re-analysis of an archival pulsar survey, resulting in the discovery of 11 new RRATs, which we described in Keane et al. (2010) (K+10 from herein), and several other authors have performed successful searches also (see § 5 which provides a census of known sources). We describe, in § 2, the methods used, and difficulties encountered, in obtaining coherent timing solutions for these sources. As well as identifying some further discoveries in § 3, we present followup observations of the new RRATs we previously identified. We have been able to obtain solutions for seven sources, described in § 4, which doubles the number of RRAT timing solutions that are known. We discuss the importance of timing solutions, including what they allow us to infer about the neutron stars, the ability to monitor for glitch activity (which has been seen but whose significance is yet to be appreciated; see § 5.4), and important benefits such as vastly improved astrometry. In § 5 we review what is now known about neutron stars detected as RRATs, and consider the question of whether they are in any way distinct from radio pulsars, before making our conclusions in § 6.

## 2 OBSERVATIONS & ANALYSIS

### 2.1 The PMSingle Analysis

In K+10 we described our reprocessing (which we refer to as PMSingle) of the Parkes Multi-beam Pulsar Survey (PMPS), a survey of the Galactic plane between  $l = 260^\circ$  and  $l = 50^\circ$ , and  $|b| < 5^\circ$ . The survey was performed using  $96 \times 3$  MHz frequency channels centred at an observing frequency of 1374 MHz, with 250- $\mu$ s time sampling. Detailed survey specifics can be found in Manchester et al. (2001). The analysis described in K+10 resulted in the discovery of 11 new RRAT sources. We have now made an additional confirmation (see § 3.1), so that there are now 12 sources, discovered in the PMSingle analysis, which have been detected on multiple occasions. These sources have been the subject of an ongoing campaign of observations which we describe below in § 2.5 and § 4. In addition to these repeating sources, we have identified seven sources which have not been re-detected since their discovery observations. Nonetheless we consider the astrophysical nature of these sources to be self-evident, as we describe below in § 3.2 and § 3.3. These 19 sources, added to the 11 identified in McLaughlin et al. (2006) mean that there have now been 30 such transient radio sources discovered in the PMPS. The detection statistics of the PMSingle discoveries are given in Table 1, and Figure 1 shows where these sources lie in the “transient phase space” defined by Cordes et al. (2004).

### 2.2 Pulsar Timing

Pulsars are commonly referred to as stable astrophysical clocks. However, even though they are rotationally stable, on a period-by-period basis the pulses we detect from pulsars are variable in amplitude, phase and shape. These individual pulses (aka sub-pulses) can vary in random, as well as highly ordered, ways. Sub-pulse drifting is a phenomenon whereby the rotational phase wherein we see pulsar emission changes periodically (see e.g. Weltevrede et al. (2006)). Some pulsars also exhibit ‘mode-changing’, or ‘moding’, whereby they are seen to switch between two or more different stable emission profiles (Bartel et al. 1982). Another phenomenon is nulling, which can be seen as an extreme example of moding, where one of the modes shows no radio emission, i.e. the radio emission ceases and the pulsar is ‘off’ (e.g. Backer (1970)). Random changes are usually labelled as ‘pulse jitter’, e.g. the Gaussian variations in pulse phase seen in PSR J0437–4715 (Cordes & Shannon 2010). We will discuss these phenomena again in § 5. For the purposes of ‘timing’ a pulsar, i.e. modelling its rotational phase as a function of time with respect to pulsar and astrometric parameters, these variations all amount to ‘timing instabilities’. We note that none of these effects are symptomatic of *rotational* irregularities — the pulsar is still spinning down in a well-behaved manner. What is variable/unstable is the source of the radio emission. There are also rotational instabilities known as glitches which are single events consisting of instantaneous jumps in rotation frequency and its derivatives (see e.g. Espinoza (2009); Espinoza et al. (2011)). Additionally, the possibly more general phenomena of slow-down rate switching may be occurring in much of the pulsar population (Lyne et al. 2010), something which we consider further in § 5.

### 2.3 Integrated Profiles

To perform ‘pulsar timing’ of a source it is usually observed for a large number of contiguous pulse periods, which are integrated to create an average pulse profile  $P(t)$ . The addition of many pulse periods is performed for two reasons: (1) to compensate for all of the timing instabilities outlined above, and (2) to increase the signal-to-noise ratio of  $P(t)$ . We note that a high signal-to-noise ratio does not imply a stable profile (we define stability below). In practise, as many periods as possible are used in timing ‘normal’/‘slow’ pulsars, typically  $10^2$ – $10^3$ , but for the faster millisecond pulsars (MSPs)  $\gtrsim 10^5$  are used routinely. Determining a pulse time-of-arrival (TOA) for a given observation then amounts to cross-correlating the observed profile  $P(t)$  with a very high S/N (or sometimes even analytic) template profile  $T(t)$  under the *assumption* that the profile is just a shifted, scaled and noisier version of the template, i.e.

$$P(t) = AT(t + \psi) + N(t), \quad (1)$$

where  $A$  is a scale factor,  $\psi$  is a phase shift and  $N$  is an additive noise term (Taylor 1990). Determining  $\psi$  gives the TOA relative to some known reference time, usually the observatory clock.

Equation (1) is valid if the profile is stable. For a profile to be stable its correlation coefficient with the template,  $R = R(n)$ , must improve according to  $\langle 1 - R(n) \rangle \propto n^{-1}$

**Table 1.** The observed properties of the newly identified sources from the PMSingle analysis, as well as those BB10 candidates which we have confirmed. Note that for sources previously published in K+10 the DM values are no more precise due to a lack of multi-frequency observations, necessary for accurately determining DM. The distances quoted are those derived from the DM using the NE2001 model of the electron content of the Galaxy (Cordes & Lazio 2002), with typical errors of 20 percent. The quoted 1.4-GHz peak flux densities are determined by using the radiometer equation (Lorimer & Kramer 2005) and using the known gain and system temperature of the 20-cm multi-beam receiver (as given in the April 6, 2009 version of the Parkes Radio Telescope Users Guide) and have typical uncertainties of 30 percent level. The † denotes the fact that J1652–44 has been detected in just 1 of 28 observations as a single pulse source. It is detected in 22 of these observations as a folded source. The ‡ denotes two sources for which a detection has recently been reported in the HTRU survey (Burke-Spolaor et al. 2011b)

Source	DM (cm <sup>-3</sup> pc)	D (kpc)	P (s)	w (ms)	$S_{\text{peak}}$ (mJy)	$L_{\text{peak}}$ (Jy kpc <sup>2</sup> )	$N_{\text{det}}/N_{\text{obs}}$	$N_{\text{pulses}}$	$T_{\text{obs}}$ (hr)	$\dot{\chi}$ (hr <sup>-1</sup> )
<b>Repeating sources</b>										
J1047–58	69.3(3.3)	2.3	1.231	4	630	3.3	7/28	60	16.0	3.8
J1423–56‡	32.9(1.1)	1.3	1.427	5	930	1.5	13/22	48	15.0	3.2
J1514–59	171.7(0.9)	3.1	1.046	3	830	7.9	32/32	361	19.2	18.7
J1554–52	130.8(0.3)	4.5	0.125	1	1400	28.3	37/37	703	13.5	52.0
J1652–44	786(10.0)	8.4	7.707	64	40	2.9	1/28†	9	13.1	0.7
J1703–38	375(12.0)	5.7	-	9	160	5.1	13/18	25	14.1	1.7
J1707–44	380(10.0)	6.7	5.764	12	575	25.8	26/27	129	14.4	8.9
J1724–35	554.9(9.9)	5.7	1.422	6	180	5.8	17/23	49	14.9	3.2
J1727–29	92.8(9.4)	1.7	-	7	160	0.4	4/11	4	6.1	0.6
J1807–25	385(10.0)	7.4	2.764	4	410	22.4	25/25	149	18.1	8.2
J1841–14	19.4(1.4)	0.8	6.598	3	1700	1.0	42/43	989	15.6	63.4
J1854+03	192.4(5.2)	5.3	4.558	16	540	15.1	29/32	146	16.3	8.9
<b>Non-repeating sources</b>										
J0845–36	29(2)	0.4	-	2	230	0.04	1/2	1	1.1	1.8
J1111–55	235(5)	5.6	-	16	80	2.5	1/7	2	4.3	0.4
J1308–67‡	44(2)	1.2	-	2	270	0.4	1/5	2	3.1	0.6
J1311–59	152(5)	3.1	-	16	130	1.3	1/6	1	3.3	0.3
J1404–58	229(5)	4.8	-	4	220	5.1	1/10	7	6.1	1.1
J1649–46	394(10)	5.1	-	16	135	3.5	1/4	1	3.4	0.3
J1852–08	745(10)	~ 500000	-	7	410	~ 10 <sup>7</sup>	1/9	1	4.2	0.2
<b>BB10 RRATs</b>										
J0735–62	19(8)	0.9	4.865	2	580	0.5	3/6	36	1.9	18.9
J1226–32	37(10)	1.4	6.193	12	590	1.2	13/20	112	5.8	19.2
J1654–23	74.5(2.5)	2.0	0.545	1	1300	5.2	13/14	151	2.6	57.9

where  $n$  is the number of periods averaged over to make the template (Liu et al., in preparation). In practise this is realised only after we have averaged some critical number of periods to make a profile. For smaller values of  $n$ ,  $\langle 1-R \rangle$  will improve faster than  $n^{-1}$ . Breaks in  $\langle 1-R \rangle$  at certain values of  $n$  indicate periodic instabilities, e.g. drifting and nulling timescales. Beyond some value  $n_{\text{crit}}$ , when  $\langle 1-R(n) \rangle \propto n^{-1}$  we say that  $P(t)$  is stable. We note that it has, in the past, been suggested that  $\langle 1-R(n) \rangle \propto n^{-0.5}$  signalled stability (Helfand et al. 1975; Rathnasree & Rankin 1995; Lorimer & Kramer 2005)<sup>1</sup> but this is incorrect. For MSPs, this critical number of periods is  $\lesssim 10^4$  and is always reached so that precision timing can be performed. In the case of slower pulsars the stability criterion is not reached (Helfand et al. 1975; Rathnasree & Rankin 1995), nor is the precision as high given that the TOA error  $\sigma_{\text{TOA}} \propto W^{3/2} P^{-1/2}$  is larger for slow pulsars than for MSPs, where  $W$  and  $P$  are the pulse width and period, respectively. Furthermore the slower pulsars are observed to exhibit more glitches and more so-

called ‘timing noise’<sup>2</sup>. Thus MSPs can be timed with very high precision whereas slow pulsars cannot.

## 2.4 Single Pulses

RRATs are generally detected via their sporadic single pulses as (by definition) they are only, or more easily, detectable in this way as opposed to methods relying on time-averaged flux. Their pulses are not detectable every rotation period and the typical observed pulse-to-pulse separations range from  $\sim 10$  to  $\sim 1000$  periods so that, unlike typical pulsars, we do not see strong pulse profiles after folding. This means we lose the two advantages of phase folding — stable profiles and increased signal-to-noise ratio. However the single pulses themselves are quite strong with typical peak flux densities of  $\sim 10^2 - 10^3$  mJy (see Table 1) and for the observations reported here the typical signal-to-noise ratios this corresponds to a range from as low as 6 to as high as 60 so that, from a signal intensity point of view, timing RRATs from their single pulses is possible. However, the single pulse

<sup>1</sup> Furthermore, in the past, arbitrary criteria for ‘stability’ have been set, e.g. Helfand et al. (1975) defined stability as  $R = 0.9995$ .

<sup>2</sup> Timing noise is a red noise feature seen in pulsar timing residuals which may be related to pulsars switching between two spin-down rates (Lyne et al. 2010).

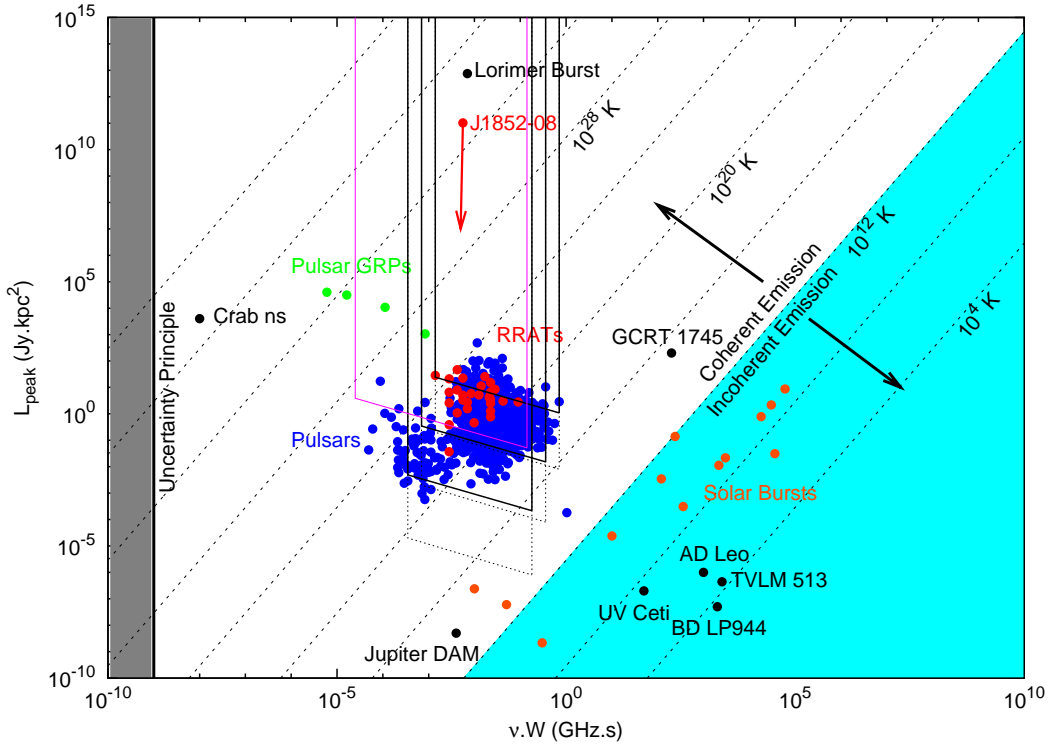


**Figure 1.** The transient ‘phase space’ with known sources identified. This is simply a plot of the radio (pseudo-)luminosity  $L = SD^2$  versus  $\nu W$ , where  $S$  is flux density,  $D$  is distance,  $\nu$  is observing frequency and  $W$  is pulse width. As radio frequencies are in the Rayleigh-Jeans regime ( $h\nu \ll kT$ ) we can draw lines of constant *minimum* brightness temperature  $T_B = 4 \times 10^{17} (SD^2/\text{Jy kpc}^2)(\text{GHz s}/\nu W)^2$  (see Keane (2010a) or Keane (2010b)). Plotted are pulsars (Hobbs et al. 2004), ‘RRATs’, pulsar ‘giant radio pulses’ (Cognard et al. 1996; Romani & Johnston 2001), flare stars (Bastian 1994; Richards et al. 2003; Osten & Bastian 2008; Osten 2008), auroral radio emission from the Sun and planets (Dulk 1985; Zarka 1998), GCRT 1745–3009 (Hyman et al. 2006) and the so-called ‘Lorimer burst’ (Lorimer et al. 2007), which we give only as a representative but not exhaustive list of sources. The boundary between coherent and incoherent emission is at  $\approx 10^{12}$  K, due to inverse Compton cooling (Redhead 1994). The sensitivity of the PMSingle analysis (black lines) to individual bursts, is overplotted, from lowest to highest  $L$ , for distances of 0.1, 1 and 10 kpc respectively. With the effective area of the SKA the curves become lower by  $\gtrsim 2$  orders of magnitude in  $L$  (dotted lines). The LOFAR survey sensitivity curve (pink line) for a distance of 2 kpc is also shown.

profiles are far from stable in phase. Phase stability is usually implicitly assumed (in timing analysis software) when using high S/N profiles and templates. This assumption is inappropriate for single-pulse timing (as it is for slow pulsars timed using unstable average profiles) and will result in extra scatter in our timing residuals with a magnitude given by the size of the phase window wherein we see single pulses. As we will show this effect is clear in our data (see Figure 4, as well as Figure 1a of Lyne et al. (2009)).

## 2.5 Observations & Timing

Here we outline the steps involved in progressing from a telescope signal to barycentred pulse arrival times and a coherent timing solution.

(i) *Observe sources in ‘search mode’.* The followup observations at Parkes consist of sporadic observations between October 2008 and March 2009, and regular approximately monthly observations since April 2009, which are ongoing. In our observational setup we utilise a bandwidth of 256 MHz divided into 512 channels, sampled every 100  $\mu\text{s}$ . The telescope receives dual linear polarisations but these are

summed to produce total intensity, i.e. Stokes I. The data are 1-bit digitised before being written to tape. The beginning of the observation is time-stamped according to the observatory clock, and is known to an accuracy of  $\sim 80$  ns.

(ii) *Search the data for single pulses.* As described in K+10 the data are searched for strong, dispersed single pulses of radiation. Once detected, dedispersed single pulse profiles, are extracted from the data.

(iii) *Obtain TOAs.* The templates used here are empirical and derived from smoothing each source’s strongest observed pulse which results in simple one component templates. Averaging all of the (detected) individual pulses gives a wider pulse profile unsuitable for cross-correlating with individual pulses. The profiles are cross-correlated with the template and  $\psi$  determined to obtain the TOA at the telescope, i.e. the site arrival time (SAT, aka topocentric arrival time), which is referenced to the time stamp.

(iv) *Convert SATs to BATs.* SATs are measured in Coordinated Universal Time (UTC). These are converted to barycentric arrival times (BATs), i.e. arrival times at the solar system barycentre at infinite frequency (with dispersive delay removed) in Barycentric Coordinate Time (TCB). The steps involved in this conversion, and definitions of

these time systems are well described elsewhere (Lorimer & Kramer 2005, Hobbs et al. 2006; Edwards et al. 2006, or see Appendix E of Keane 2010).

Once we have obtained BATs we can model the timing parameters of the source. This is done using PSRTIME<sup>3</sup> and TEMPO<sup>2</sup><sup>4</sup>, standard pulsar timing software packages. If we express the rotational frequency of the pulsar as a Taylor expansion

$$\nu(t) = \nu_0 + \dot{\nu}_0(t - t_0) + \frac{1}{2}\ddot{\nu}_0(t - t_0)^2 + \dots, \quad (2)$$

the rotational phase (simply the integral of frequency with respect to time, modulo  $2\pi$ ) is given by

$$\begin{aligned} \phi(t) = \phi_0 + \nu_0(t - t_0) + \frac{1}{2}\dot{\nu}_0(t - t_0)^2 \\ + \frac{1}{6}\ddot{\nu}_0(t - t_0)^3 + \dots \quad (\text{mod } 2\pi). \end{aligned} \quad (3)$$

In addition to these terms, binary effects should be added (however none of the sources discussed here have detected binary companions) and the *observed* phase will be different due to positional uncertainties. Timing consists of minimising the  $\chi^2$  of the residuals of our timing model, i.e. the difference between our model for when pulses arrive and when they actually arrive (the BATs we measure).

Immediately after discovering and confirming a new source we know very little about it. If the rate of pulse detection is too low then we will not be able to determine an estimate of the period using period differencing. In this case there is no way to proceed with timing the source. Assuming the rate is sufficient then we have an initial guess for the period and a knowledge of the sky position (uncertain to  $\sim 7$  arcmin in both right ascension and declination, corresponding to the beamwidth of a pointing in the PMPS) which serves as our initial guess of the timing ephemeris. We can see from Equation 3 that different effects will become visible in our residuals over different timescales. On the shortest timescale all we need to worry about is the rotation frequency,  $\nu$ . We begin our timing solution by obtaining several closely spaced ‘timing points’, (say) every 8 hours over the space of a day or two. This is necessary to build a coherent solution on short timescales as our initial knowledge of the period is not sufficient to be able to combine, in phase, TOAs obtained a few days apart. Once this has been done the period will be known to sufficient accuracy that all our TOAs over the timescale of a few days will be in phase. If we monitor the source like this we will notice a quadratic signature appear in our residuals. This is the effect of the frequency derivative  $\dot{\nu}$  (which is initially set to zero). For the sources reported here, this  $\dot{\nu}$  effect is seen over a timescale of weeks to months. Positional uncertainties result in sinusoids, with periods of one year, appearing in the residuals. If the sky position is not well known, it is difficult to disentangle the effects of spin-down rate and positional uncertainty until at least 6 months of monitoring has been made, and preferably at least one year (i.e. a quadratic curve is highly covariant with half a sine wave).

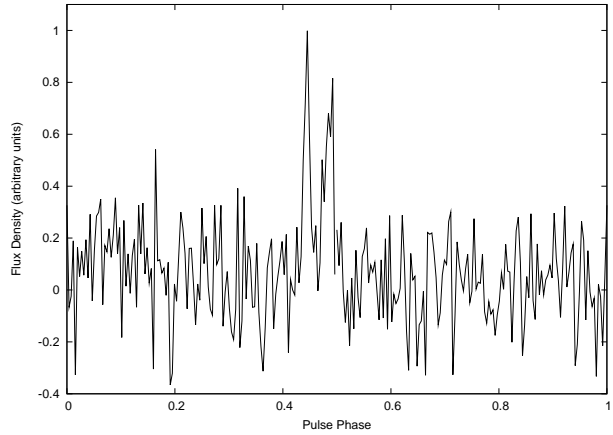


**Figure 2.** A typical pulse profile from a 30-minute observation of J1652–44.

### 3 NEW DISCOVERIES

#### 3.1 J1652–44

J1652–44 was one of the Class 1 candidates found in the analyses presented in K+10. Despite showing 9 strong pulses in its discovery observation, confirmation was difficult. A small number of bursts have since been observed but none as strong as in the original survey observation. These borderline detections were not enough to conclusively confirm the candidate but it turned out that J1652–44 was sometimes detectable by folding the time series at the period of the pulsar. Looking for a folded signal was made possible by obtaining an initial period of  $P = 7.70718$  s from period differencing of the discovery burst times of arrival (TOAs, see K+10 for a description of this). Using this, and the dispersion measure (DM) at which the bursts peaked, as a starting point, each of 28 followup observations were folded and dedispersed into archives consisting of 1-minute subintegrations. A search in period and DM was then performed using PDMP<sup>5</sup>. In 22 of the observations a folded signal, like that shown in Figure 2, was detected with a double-peaked profile.

#### 3.2 Single Detections

Additionally, we have identified 6 of the PMSingle candidates which we consider to be ‘self-confirmed’, i.e. we have not re-observed bursts in our followup observations but we deem the survey detection sufficiently convincing that the astrophysical nature of these sources is clear. A number of these are just single bursts, showing the characteristic dispersive delay expected from celestial sources, are detected in only one of the 13 beams and show no signatures of RFI. Figure 3 shows an indicative frequency versus time plot demonstrating the dispersive sweep of an individual pulse. We note that unlike the bursts reported by Burke-Spolaor et al. (2011a), whose origin appears to be terrestrial, no

<sup>3</sup> <http://www.jb.man.ac.uk/~pulsar/observing/progs/psrtime.html>

<sup>4</sup> <http://www.atnf.csiro.au/research/pulsar/tempo2/>

<sup>5</sup> <http://psrchive.sourceforge.net/manuals/pdmp>

“kinky” deviations are seen from the ideal dispersion law, nor are any of these events detected in multiple beams.

The sources show between one and seven pulses in their discovery observations and have been followed up for between one and six hours, without showing further pulses. As these bursts are just a few milliseconds in duration a neutron star is expected to be the source of the emission. As the discovery observations clearly show these sources to be astrophysical, the long followups with no confirmation suggest a very low rate of bursting. They therefore have significant implications for the population size of such sources. For instance, if a source shows one burst in 5 hours of observation, it suggests that, as a zeroth order estimate,  $\sim 9$  such sources may have been missed during the survey which consisted of 35-minute pointings. In this sense then, the longer these sources remain unconfirmed the more interesting they are. For those sources which have shown just one burst (J0845–36, J1311–59, J1649–46 and J1852–08) we cannot rule out some theoretically predicted explanations which would not be expected to repeat, e.g. annihilating mini black holes (Rees 1977), supernovae (Phinney & Taylor 1979) or merging neutron star binaries (Hansen & Lyutikov 2001). Observing repeated bursts rules out such events and points at a temporarily re-activated ‘dead’ pulsar as a likely origin.

### 3.3 J1852–08

The most interesting single pulse source is J1852–08, an isolated 7-ms pulse with a dispersion measure of  $745 \text{ cm}^{-3} \text{ pc}$  (see Figure 3). Dividing the band into 8 sub-bands and obtaining TOAs for each shows a frequency dependent-delay between each TOA of the form  $f^{-\alpha}$  where  $\alpha = 2.02(1)$ , consistent with the theoretical value of 2 for a cold ionised inter-stellar medium. Hence the pulse is unlikely to be due to a terrestrial source. We note that the half-amplitude pulse width is slightly wider in the bottom half of the band, at 9.1 ms compared to 7.1 ms in the top half of the band, although there is no obvious indication, permitted by the signal-to-noise ratio, of scattering, e.g. an exponential tail, so that this may be intrinsic to the pulse. Dedispersing the entire band gives a pulse width of 7.3 ms. We note that the empirical model of Bhat et al. (2004) predicts a scattering time of  $\sim 130$  ms, which is not seen here, where the scattering time can be no more than a few milliseconds. However this empirically determined relation between scattering, DM and observing frequency has observed deviations of more than an order of magnitude in either direction.

The Galactic coordinates of this source are  $l = 25.4^\circ$ ,  $b = -4.0^\circ$ , so that this large DM implies an extragalactic distance for this source. According to the NE2001 Galactic electron density model (Cordes & Lazio 2002) the maximum contribution from the Galaxy along this line of sight is  $DM_{\text{Gal}} = 533 \text{ cm}^{-3} \text{ pc}$ . Thus a Galactic explanation of this source requires that the NE2001 model is incorrect along this line of sight. If there were an unknown contribution to the free electron density,  $DM_{\text{Gal}}$  would increase, and the inferred distance to J1852–08 could be drastically reduced (see Deller et al. (2009) for a discussion of errors in NE2001 distances). In that case the burst from J1852–08 would appear to be a giant radio pulse from a pulsar. However for typical giant radio pulse distributions (see e.g. Karuppusamy

et al. (2010)) this means that we would already have detected many weaker pulses, which is not the case.

If NE2001 is reliable along this line of sight then the surplus of  $DM_{\text{extra}} = 222 \text{ cm}^{-3} \text{ pc}$  must be due to extragalactic contributions (the inter-galactic medium and any putative host galaxy). A DM-redshift relation is known (Ioka 2003) which would apply to this component, and takes the form:  $DM_{\text{extra}} \approx 1200z \text{ cm}^{-3} \text{ pc}$ . If all of the  $DM_{\text{extra}}$  component is due to the inter-galactic medium, the inferred redshift and distance are  $z \approx 0.18$  and  $D \approx 520h^{-1} \text{ Mpc}$  ( $\Omega_m = 0.3$ ,  $\Omega_\Lambda = 0.7$ ). Allowing for a contribution of  $100 \text{ cm}^{-3} \text{ pc}$  from a host galaxy (see Lorimer et al. (2007)), these values become  $z \approx 0.09$  and  $D \approx 260h^{-1} \text{ Mpc}$ . This implies the strongest intrinsic peak luminosity of all the PMPS sources, of  $\gtrsim 10^{11} \text{ Jy kpc}^2$ . It is noticeable as the RRAT with the highest peak luminosity in Figure 1 where it lies just below the burst reported by Lorimer et al. (2007) in transient phase space, and some 6 orders of magnitude above the giant pulses seen in some radio pulsars. The SIMBAD<sup>6</sup> database lists no apparent host galaxies for this object, although the positional uncertainty for this event is quite large, at  $\sim 7$  arcmin. Furthermore, as this event occurred in June 2001, just like the Lorimer burst, which occurred two months later, this burst was a pre-LIGO and pre-GEO600 event, so no gravitational wave emitting counterpart can be searched for. We can say that, by causality and the pulse duration, the source is limited to a maximum size of 2100 km. Thus, if the NE2001 model is correct along this line of sight, J1852–08 fits many of the criteria for being a second example of the Lorimer burst.

### 3.4 Repeating Sources (BB10)

In addition to the PMPS, two further pulsar surveys have been performed at the same Galactic longitudes, but at intermediate and high Galactic latitudes of  $5^\circ < |b| < 30^\circ$  (Edwards et al. 2001; Jacoby et al. 2009). These surveys used the same specifications as the PMPS, except with a faster time sampling of  $125 \mu\text{s}$  and shorter pointings of 4.4 minutes. Recently, Burke-Spolaor & Bailes (2010) (BB10 from herein) have analysed these surveys and presented 14 new transient sources, 7 of which were candidates which had never been confirmed. One of these unconfirmed sources was in fact re-detected by the authors soon after their publication (Burke-Spolaor, private communication), but 6 remained unconfirmed. As part of our observing programme, these 6 sources were observed in search of single pulses and 3 of these have now been confirmed. Two of these sources have been regularly observed since January 2010 and both have provisional timing solutions, which we describe further in § 4.2.

## 4 NEW TIMING SOLUTIONS

After discovery of a new source, very little is known: a dispersion measure, a crude knowledge of the position, and perhaps a period. Determining a timing solution increases our knowledge greatly. It enables us to infer properties of the

<sup>6</sup> <http://simbad.u-strasbg.fr/simbad/>

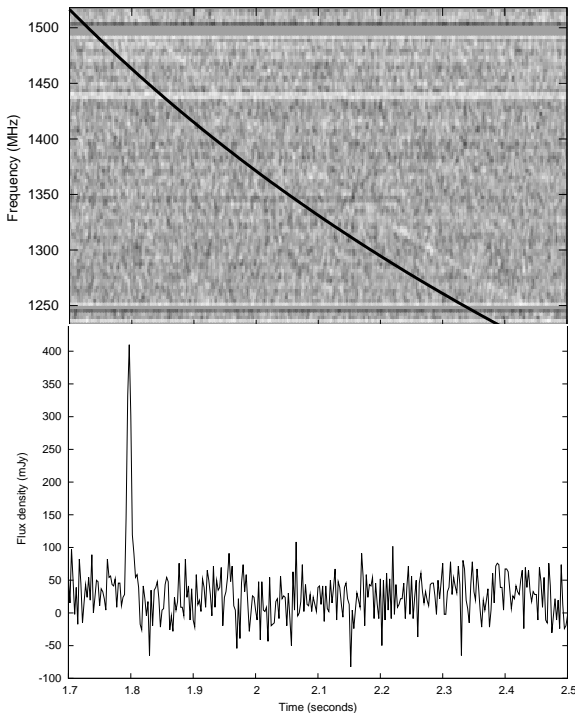


**Figure 3.** (Top) A plot of the J1852–08 burst in frequency-time space, aka a ‘dynamic spectrum’. The theoretical dispersion law is  $t_{\text{delay}} = 4150 (DM/f^2)$  sec, where  $DM$  is the dispersion measure in units of  $\text{cm}^{-3} \text{pc}$  and  $f$  is the observing frequency in MHz. The offset black solid line is the theoretical curve for a source with  $DM = 745 \text{ cm}^{-3} \text{pc}$ , which is clearly obeyed by the pulse. (Bottom) The dedispersed pulse, i.e. the dynamic spectrum collapsed along a slope given by the theoretical curve. The flux density scale is uncertain by up to 30 percent.

star, such as energy-loss rate, magnetic field strength and evolutionary timescales (see e.g. Lyne & Smith (2004)). We report these values for the PMPS RRATs in Table 3 and Figure 5. Timing solutions also tell us where in  $P - \dot{P}$  space our sources occupy, allowing us to investigate and/or infer pulsar evolutionary paths. Furthermore we can identify additional contributions to pulsar spin evolution, in particular due to glitches, which manifest as step changes in spin frequency and its derivatives (see e.g. Espinoza et al. (2011)). The accurate astrometry provided by the timing solutions allow multi-wavelength observations (see e.g. Dhillon et al. (2011)), impossible with the poor spatial resolution of single-dish radio telescopes. Another spin-off is that an improved retrospective search for pulses will be possible, allowing an optimal nulling analysis.

Here we report the complete timing solutions for seven PMSingle sources. These solutions consist of fits in period, period derivative, right ascension and declination. Figure 4 shows the timing residuals for 6 of these sources (those timed via their single pulses, all but J1652–4406) and Table 2 gives the parameters of the fits. Below we quickly review each of the sources in turn, before giving updates on provisional timing solutions of PMSingle and BB10 sources which do not yet have a timing solution.

#### 4.1 Complete Timing Solutions

J1513–5946 (formerly J1514–59) is detected in all 30 observations, totalling 18 hours. The periodic nulling described in K+10 is detected in every observation. During the ‘on’ periods, J1513–5946 is detectable in a periodicity search. Figure 4 shows its timing residuals where we can clearly see two bands, symptomatic of two pulse components. Removing this banding, i.e. simply applying a jump between the two bands, as done for J1819–1458 in Lyne et al. (2009), we obtain a timing solution with  $\chi^2/n_{\text{free}} = 4.2$ . The fact that this is not equal to 1 is expected due to our fundamental violation of the stable profile assumption (see § 2.3) and is due to the intrinsic variability of the single pulses, i.e. they are variable in both phase and pulse width. The ‘on’ times are not long enough, at  $\sim 1$  minute, to be able to form stable profiles and result in fewer TOAs with lower error bars, but with the same scatter as shown in Figure 4. The timing solution places J1513–59 amongst the ‘normal’ pulsars in the  $P - \dot{P}$  diagram (see Figure 6), with perhaps a slightly higher than average magnetic field strength.

J1554–5209 (formerly J1554–52) is also detected in all observations, totalling 13 hours. The timing residuals show three clear bands, which, upon removal, gives us a timing solution with  $\chi^2/n_{\text{free}} \sim 10$ , which we again attribute to the intrinsic variability in the single pulses. In units of pulse periods it has by far the largest scatter in its residuals. J1554–5209 is also occasionally detectable in periodicity searches, although with less significance. It has been common (see e.g. Deneva et al. (2009)) to define a quantity  $r = (S/N)_{\text{SP}}/(S/N)_{\text{FFT}}$ , the ratio of the single pulse search to FFT search signal-to-noise ratios. For J1554–5209, each observation so far has had  $r > 1$ . It is noticeable in Figure 6 as the outlying PMSingle source with the lowest period, and the highest  $\dot{E}$  in our sample. It has a typical magnetic field for a pulsar and with  $\tau = 0.9$  Myr it is the second ‘youngest’ PMSingle source.

J1652–4406 is a radio pulsar with a very large rotation period of  $P = 7.707$  s. In fact, J1652–4406 is the third slowest radio pulsar known, just behind J1001–5939 ( $P = 7.73$  s) and J2144–6145 ( $P = 8.51$  s). As discussed in § 3.1, we have been able to confirm this source since the discoveries announced in K+10. Although initially identified as a source showing strong single pulses, we have confirmed it as a periodic source. It is detected in 22 of 28 followup observations in this way, but never convincingly re-detected in a search for single pulses. Figure 2 shows a typical detection. From these observations, a timing solution has been obtained with  $\chi^2/n_{\text{free}} = 0.75$ . The resultant  $\dot{P}$  places J1652–4406 just above the death line, just like J1840–1419, but for this source, unlike J1840–1419, there is little prospect of high energy followup as it is towards the Galactic centre, with  $l = 341.56^\circ$ ,  $b = 0.09^\circ$  and with  $DM = 786 \text{ cm}^{-3} \text{pc}$  has an inferred distance of 8.4 kpc (Cordes & Lazio 2002). At 10 times further distance we expect 100 times less X-ray flux than from J1840–1419, but the situation is likely to be even worse given the extra absorption that would result from the large neutral hydrogen density in the Galactic centre.

J1707–4417 (formerly J1707–44) has been detected in all but one of 23 observations which have totalled 13 hours. The timing residuals show two clear bands, separated by

$\sim 200$  ms. There are no other pulses detected between these two bands although there are instances where both pulse components are seen together. This suggests that the active emission time is longer than the time which the emission beam spends in our line of sight. This is consistent with both the ‘patchy beam’ (Lyne & Manchester 1988), and ‘hollow cone’ (Rankin 1993) beam models. Removing the banding effect, the timing solution we determine is remarkably good with  $\chi^2/n_{\text{free}} = 1.1$ , indicating that the single pulses are very stable in phase and pulse width. J1707–4417 is an old neutron star with  $\tau = 7.8$  Myr and lies quite close to the death line, just above J1840–1419, in the  $P - \dot{P}$  diagram.

J1807–2557 (formerly J1807–25) is detected in all observations covering a total of 16 hours. The timing residuals do not show any obvious banding, although there is a slight suggestion of a second band (see Figure 4). The scatter in the residuals is quite large and the fit has  $\chi^2/n_{\text{free}} \sim 20$ . Evidently the single pulses from this source are quite variable in phase. We can also see that the error bars in the TOAs vary considerably in extent, indicating that the shape and/or the strength of the individual pulses varies appreciably between detections. Just as for J1707–4417 and J1840–1419, it is an old neutron star with  $\tau = 8.8$  Myr.

J1840–1419 (formerly J1841–14) has a large burst rate with strong single pulses detected at a rate of approximately one per minute. It can usually be detected in periodicity searches but with less significance than single pulse searches. Just as for J1707–4417, it has an exceptionally good timing solution with a  $\chi^2/n_{\text{free}} = 1.5$ , indicating that its single pulses are very stable in shape and in phase. The proximity of this old pulsar allows the prospect of X-ray observations. We have recently performed such observations using *Chandra* and we will report the results of these observations elsewhere. J1840–1419 lies just above the radio death line and, as such, studies of this star will help us to investigate important questions concerning old, dying pulsars.

J1854+0306 (formerly J1854+03) has been detected in 28 of 31 observations during 16 hours of followup. The timing solution has  $\chi^2/n_{\text{free}} \sim 40$  and we can see in Figure 4 that the observed scatter is much larger than the error bars of individual TOAs, indicating variability in pulse phase. The pulse widths are not seen to vary to the same degree. Of the PMSingle sources, J1854+0306 has the strongest magnetic field, the second strongest of all the RRAT sources with determined  $B$ , behind J1819–1458 (see Table 2).

For completeness, Table 2 also lists the 11 PMPS RRATs discovered in the PMPS and reported in M+06. Since the discovery of these sources, followup timing observations have been performed, primarily at Parkes, but also at the GBT, Arecibo and Jodrell Bank (McLaughlin et al. 2009; Lyne et al. 2009). Of these 11, there are seven for which timing solutions have been obtained are given in the table.

## 4.2 Preliminary/Unsolved Sources

In addition to the 14 PMPS sources now with coherent timing solutions there are nine others which have been re-detected on multiple occasions but do not yet have a coherent timing solution. We review the status of these in turn.

J1047–58 is a very sporadic source, whose rate of detected bursts varies between extremes an order of magnitude higher and lower than its average rate of  $\sim 4 \text{ hr}^{-1}$ . This re-

**Table 3.** The derived quantities for the 14 PMPS surces discovered as RRATs (the ♣ and ★ denote discovery in K+10 and M+06 respectively), which now have coherent timing solutions. The interpretations of  $B$  and  $\tau$  should be made with caution, as described in § 5. The values quoted are obtained from evaluating  $B_{\text{vac}} = 3.2 \times 10^{19} \text{ G} \sqrt{P\dot{P}/\sin^2 \alpha}$ ,  $B_{\text{ff}} = 2.6 \times 10^{19} \text{ G} \sqrt{P\dot{P}/(1 + \sin^2 \alpha)}$  (with  $\alpha = 90^\circ$  in both cases),  $\tau = P/\dot{P}$  and  $\dot{E} = 4\pi^2 I \dot{P} P^{-3}$  (see e.g. Lyne & Smith (2004); Spitkovsky (2006)).

Source	$B_{\text{vac}}, B_{\text{ff}}$ ( $10^{12} \text{ G}$ )	$\tau$ (Myr)	$\dot{E}$ ( $10^{31} \text{ erg s}^{-1}$ )
J0847–4316★	25.1, 14.1	0.8	2.0
J1317–5759★	6.3, 3.5	3.2	2.5
J1444–6026★	10.0, 5.6	4.0	0.6
J1513–5946♣	3.0, 1.7	1.9	29.4
J1554–5209♣	0.5, 0.3	0.9	4605.9
J1652–4406♣	8.6, 4.8	12.8	0.1
J1707–4417♣	8.3, 4.7	7.8	0.2
J1807–2557♣	3.8, 2.1	8.8	0.9
J1819–1458★	50.1, 28.2	0.1	32.8
J1826–1419★	2.5, 1.4	1.3	79.4
J1840–1419♣	6.5, 3.7	16.5	0.1
J1846–0257★	25.1, 14.1	0.4	6.3
J1854+0306♣	26.0, 14.6	0.50	6.1
J1913+1330★	2.5, 1.4	1.6	39.8

sults in it being detected in only a quarter of observations, which has hampered efforts to determine a coherent timing solution, although a solution is expected for this source, with sufficient observation time.

J1423–56 is more stable in its burst rate than J1047–58, and although a solution is not yet determined, it is expected that this will be possible in the coming months.

J1703–38 is another source with a low burst rate of  $\lesssim 2 \text{ hr}^{-1}$ . Despite this, since its discovery in K+10, we have been able to determine a period of  $P = 6.443$  seconds using period differencing. A timing solution has not been forthcoming however as very long observations ( $> 1 \text{ hr}$ ) are needed to guarantee the detection of multiple pulses (essential for identifying the topocentric period in each observation). Higher sensitivity observations and perhaps lower frequencies (where the burst rate might be higher, as seen by McLaughlin (2009)) are planned for the future.

J1724–35 was the first PMSingle candidate to be confirmed. It has been missed in 6 of 21 followup observations which have totalled 15 hours. Furthermore, when detected its observed burst rate is  $\lesssim 3 \text{ hr}^{-1}$ , which is quite low, so that obtaining a coherent timing solution has not been possible. A renewed attempt will be made in the future to ‘solve’ this source, using higher sensitivity, again at lower frequencies, and this is planned for future work.

J1727–29 has by far the lowest burst rate of any of our confirmed sources with just 4 pulses detected in 6 hours. Further followup is not feasible given the required telescope time, as such a low rate makes determining a timing solution very difficult. In fact we have not even determined the underlying period, if any, in this source. With pulses of  $\sim 7 \text{ ms}$  wide its maximum source size is constrained to be  $\sim 2100 \text{ km}$  by causality. This is much larger than a neu-



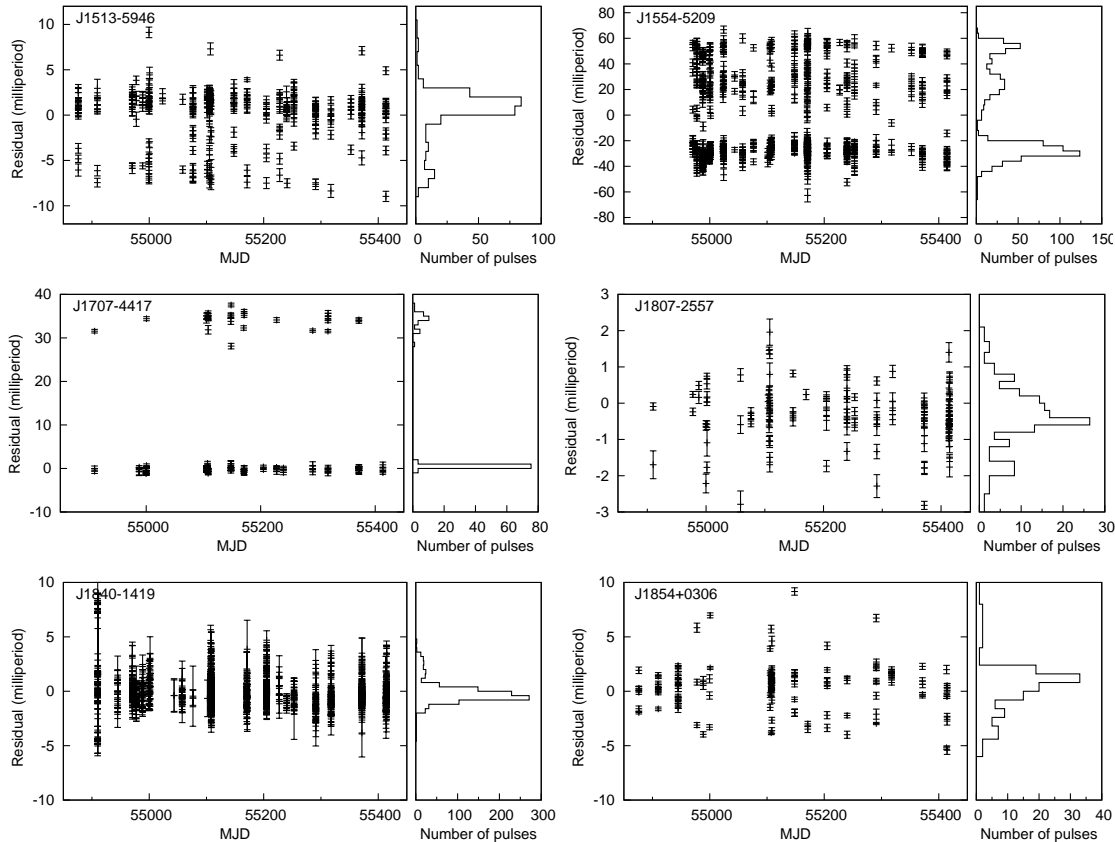


**Figure 4.** Plotted are timing residuals for the 6 PMSingle sources with determined timing solutions, via single pulse timing. From top to bottom the sources are: J1513–5946, J1554–5209, J1707–4417, J1807–2557, J1840–1419, and J1854+0306. Note the differing ranges in residual for each source. This tells us that, for example, J1840–1419 and J1707–4417 are much better single pulse ‘timers’ than J1554–5209.

tron star but less than the minimum radius for a relativistic white dwarf at the Chandrasekhar mass (Shapiro & Teukolsky 1983) so that we suspect a neutron star origin.

Of the other PMPS RRATs, we are confident that timing solutions will be obtained for J1754–30, J1839–01 and J1848–12, but it a solution for J1911+00 seems unlikely due to its very low burst rate. Of the three BB10 RRATs which we have confirmed it seems that timing solutions should be possible with continuing observations.

J0735–62 is not detected in two followup observations, each of ten minutes duration. Recently we have made a third, 30-minute observation where it was easily detected, and thus confirmed it for the first time, with 20 strong single pulses. Analysing the TOA differences we determine a topocentric period of  $P = 4.865(1)$  s, consistent with the initial estimate of  $P = 4.862$  s period published in BB10. Additionally the two non-detections support their claim that the source suffers from severe scintillation. For this reason we do not yet know if obtaining a timing solution for this source is possible using a reasonable amount of observing time, but a single lengthy observation is planned in the coming months, to investigate this very question.

In the original observation of J1226–32 only 3 pulses were detected, but this was sufficient for BB10 to derive a period of  $P = 6.193$  s. We have confirmed this candidate and have observed 45 pulses in almost 3 hours of followup, although in one third of the observations it is not detectable.

We confirm the published period, and our provisional timing solution is coherent since January 2010 and regular ongoing observations should reveal a full timing solution for this source.

The original detection of J1654–23 also consisted of just 3 pulses. We have confirmed this source and have determined a period of 0.545 s, which differs from the published estimate of BB10. This is not very surprising given their small number of detected pulses. Interestingly, the period we determine, from 106 pulses detected in 2.3 hours, is not at a different harmonic. This suggests that perhaps one of the 3 pulses initially identified was terrestrial in origin. As for J1226–32 we have a provisional timing solution, coherent since January 2010 and regular observations are ongoing.

In addition to the above three sources, we have attempted to confirm three other sources. We have observed J0923–31 and J1610–17 for 1.0 and 1.2 hours respectively but have not been able to make a confirmation. We have detected 5 weak pulses from J1753–12 at the correct DM, during 1.3 hours of observation, although we hope a more significant confirmation will come with time. We have not yet followed up these 3 sources for as long as the 3 new confirmations. This is, in some sense, by design, as these sources showed just 1, 1 and 3 pulses respectively in their discovery observations, so we decided to initially focus on the higher burst rate source (which were subsequently confirmed).

**Table 2.** The timing solutions, both complete and incomplete, of all the repeating PMPS RRAT sources, as well as the BB10 candidates which we have confirmed. Sources denoted with a ♣ are those discovered in K+10 and whose timing solutions are presented in this work. Sources denoted with a ★ are those discovered in M+06 and whose timing solutions were published in McLaughlin et al. (2009) and Lyne et al. (2009). The periods quoted for the BB10 sources are those determined from our observations. Columns 2–6 inclusive constitute the fitted values. The last column states the DM but note that this was not fit in our timing analyses as followup observations at several frequencies have not been performed. Periods marked with a † have had different values published previously. In both cases (J1754–30 and J1654–23) a mis-identification of a terrestrial radio pulse as astrophysical is to blame, as has become evident after further observations which have revealed many more pulses and the true period.

Source	RA (J2000)	DEC (J2000)	P (s)	$\dot{P}$ ( $10^{-15}$ )	PEPOCH (MJD)	Data Span (MJD)	DM ( $\text{cm}^{-3} \text{ pc}$ )
<b>Complete PMPS Timing Solutions</b>							
J0847–4316★	08:47:57.33(5)	–43:16:56.8(7)	5.9774927370(7)	119.94(2)	53816	52914–54716	292.5(0.9)
J1317–5759★	13:17:46.29(3)	–57:59:30.5(3)	2.64219851320(5)	12.560(3)	53911	53104–54717	145.3(0.3)
J1444–6026★	14:44:06.02(7)	–60:26:09.4(4)	4.7585755679(2)	18.542(8)	53893	53104–54682	367.7(1.4)
J1513–5946♣	15:13:44.78(1)	–59:46:31.9(7)	1.046117156733(8)	8.5284(4)	54909	54876–55413	171.7(0.9)
J1554–5209♣	15:54:27.15(2)	–52:09:38.3(4)	0.1252295584025(7)	2.29442(5)	55039	54970–55414	130.8(0.3)
J1652–4406♣	16:52:59.5(2)	–44:06:05(4)	7.707183007(4)	9.5(2)	54947	54850–55413	786(10)
J1707–4417♣	17:07:41.41(3)	–44:17:19(1)	5.7637770030(4)	11.65(2)	54999	54909–55371	380(10)
J1807–2557♣	18:07:13.66(1)	–25:57:20(5)	2.76419486975(4)	4.994(2)	54984	54909–55414	385(10)
J1819–1458★	18:19:34.173(1)	–14:58:03.57(1)	4.26316403291(5)	575.171(1)	53351	51031–54938	196(1)
J1826–1419★	18:26:42.391(4)	–14:19:21.6(3)	0.770620171033(7)	8.7841(2)	54053	53195–54909	160(1)
J1840–1419♣	18:40:32.96(1)	–14:19:05(1)	6.5975626227(4)	6.33(2)	55074	54909–55239	19.4(1.4)
J1846–0257★	18:46:15.49(4)	–02:58:36.0(2)	4.4767225398(1)	160.587(3)	53039	51298–54780	237(7)
J1854+0306♣	18:54:02.98(3)	+03:06:14(1)	4.5578200962(1)	145.125(6)	54944	54876–55414	192.4(5.2)
J1913+1330★	19:13:17.975(8)	+13:30:32.8(1)	0.92339055858(2)	8.6799(2)	53987	53035–54938	175.64(0.06)
<b>Preliminary/Unsolved PMPS Sources</b>							
J1047–58♣	10:47:56(55)	–58:41(7)	1.23129(1)	–	55779	–	69.3(3.3)
J1423–56♣	14:23:11(53)	–56:47(7)	1.42721(7)	–	54557	–	32.9(1.1)
J1703–38♣	17:03:26(37)	–38:12(7)	6.443(1)	–	54999	–	375(12)
J1724–35♣	17:24:43(36)	–35:49(7)	1.42199(2)	–	54776	–	555(10)
J1727–29♣	17:27:19(33)	–29:59(7)	–	–	–	–	93(10)
J1754–30★	17:54:16(33)	–30:11(7)	1.32049(1)†	–	55025	–	293(19)
J1839–01★	18:39:53(29)	–01:36(7)	0.93190(1)	–	51038	–	307(10)
J1848–12★	18:48:02(30)	–12:47(7)	6.7953(5)	–	53158	–	88(2)
J1911+00★	19:11:48(29)	+00:37(7)	6.94(1)	–	52318	–	100(3)
<b>Unsolved BB10 RRATs</b>							
J0735–62	07:35:24(63)	–62:58(7)	4.865(1)	–	55352	–	19(8)
J1226–32	12:26:50(34)	–32:27(7)	6.192997(7)	–	55000	–	37(10)
J1654–23	16:54:03(31)	–23:35(7)	0.54535972(3)†	–	55261	–	74.5(2.5)

### 4.3 PMPS Timing Status

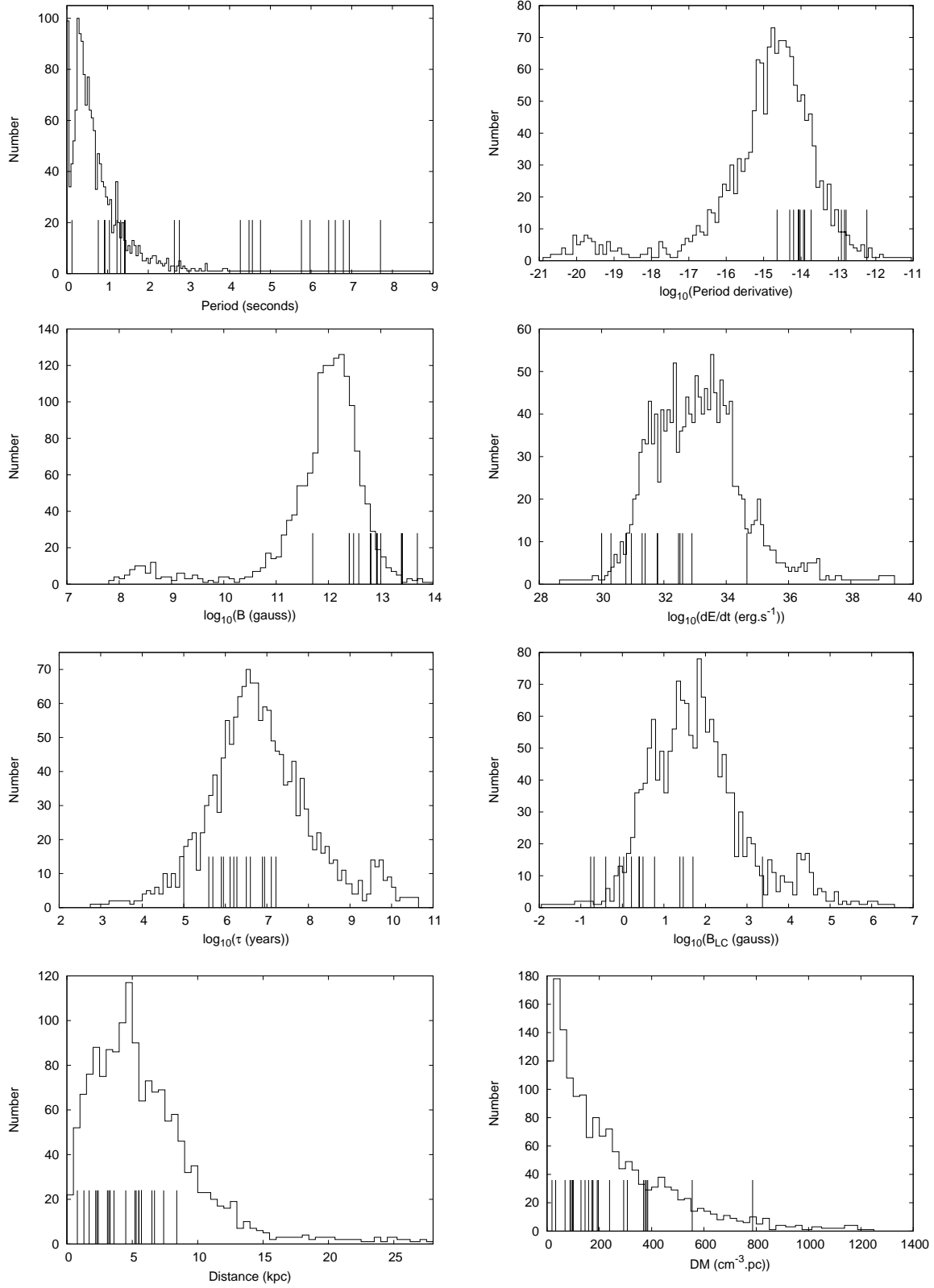
Of the 30 sources now identified in the PMPS, 23 have been re-detected on multiple occasions, of which 22 of these have known periods and 14 of these now have coherent timing solutions. Of the unsolved sources, the prospects for obtaining solutions are promising for five of these, but seem unlikely for the rest, due, primarily, to the low rate of pulse detection, i.e. an unfeasibly long observing time would be required. Additionally, two of the BB10 RRATs are expected to have full solutions in due course. We also note that these sources are the only radio neutron stars with timing solutions obtained using individual pulses, rather than averaged profiles. Figure 6 shows an up to date  $P - \dot{P}$  diagram showing all known radio pulsars, the 14 RRATs, the magnetars and the XDINSs, for which  $P$  and  $\dot{P}$  are known.

Figure 5 summarises the properties, both measured and derived, resulting from the timing analysis. The values for all PMPS RRATs are shown and contrasted with the distribution of values in the pulsar population as a whole. We can see from Figures 5 and 6 that the RRATs certainly have long periods with half of the 22 sources having periods

$P > 4$  s. The four sources with the highest inferred magnetic field strengths occupy a void region of  $P - \dot{P}$  space and J1819–1458 remains the source with the highest  $B$ . At least four other RRATs (and possibly six) of the 14 with known  $\dot{P}$  are ‘normal’. The remaining four sources have very long periods and lie just above the death line. Identification of these 3 ‘groups’ hints at an answer (or rather answers) to the question: what is a RRAT? We discuss this in detail in § 5 but it is clear that some are normal pulsars, some old/dying pulsars and some occupy the high- $B$  void region of  $P - \dot{P}$  space.

## 5 DISCUSSION

In our PMSingle analysis we have discovered 19 sources, which brings the number of PMPS RRATs known to 30. These discoveries are broadly consistent with the initial population estimate for RRATs — we removed the effects of ‘RFI blindness’ (Eatough et al. 2009), which affected  $\sim 1/2$  of the PMPS pointings, and (more than) doubled the known PMPS RRATs. In addition to the PMPS, others have iden-



**Figure 5.** In each panel we compare the properties of the known pulsar population to those of the RRATs. The parameters are  $P$ ,  $\dot{P}$ ,  $B$ ,  $\dot{E}$ ,  $\tau$ ,  $B_{LC}$ , distance and DM. Apart from  $P$ , distance and DM the abscissa is plotted as a base-10 logarithm.

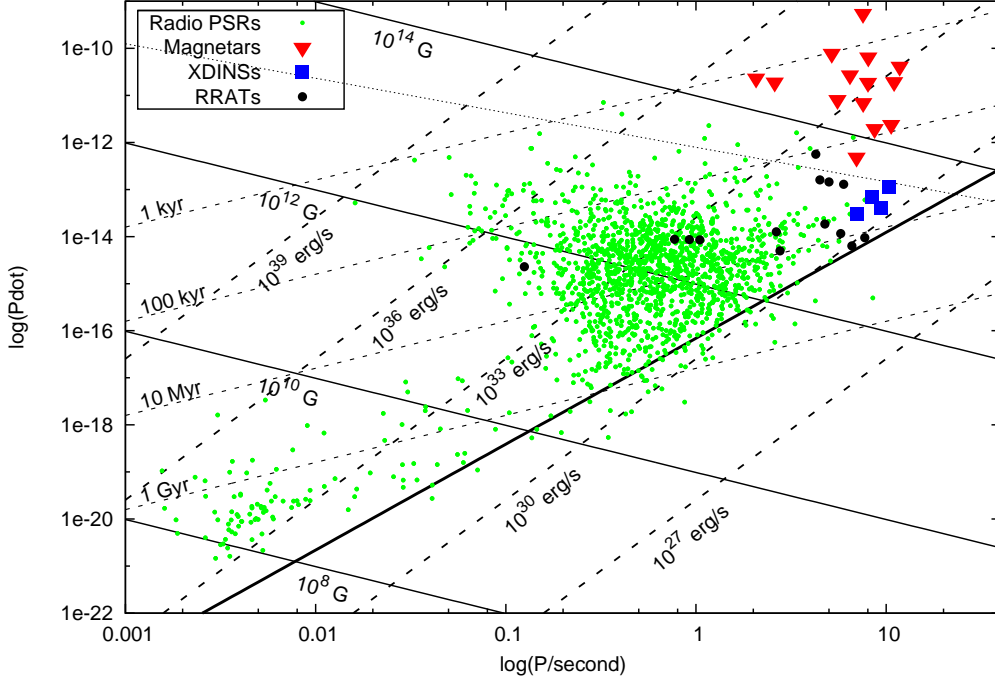


**Figure 6.** The pulsar  $P - \dot{P}$  diagram. Shown are the radio pulsars, which can clearly be seen to consist of two classes — the ‘slow’ pulsars and the MSPs, as well as those RRATs, XDINSs and magnetars with known period derivative. The region in the bottom right (bounded by the thick black line) denotes the canonical ‘death valley’ of Chen & Ruderman (1993) where we can see there is a distinct (but not complete) lack of sources. The radio loud-radio quiet boundary of Baring & Harding (1998), which divides the magnetars and the XDINSs, is also shown (dotted line) and we can see that only  $\sim 1\%$  of sources are found above this line. Also plotted are lines of constant  $\dot{E}$ ,  $B$  and  $\tau$ , calculated using the standard equations (Lyne & Smith 2004).

tified sources to be RRATs — seven at Arecibo, including J1854+0306 (Deneva et al. 2009), two at GBT (Hessels et al. 2008; Boyles et al. 2010), 25 others at Parkes (BB10, as mentioned already, as well as the first results of the HTRU survey<sup>7</sup>), one at Puschino (Shitov et al. 2009) and four at Westerbork (Rubio-Herrera 2010). In total, this amounts to 67 sources identified as RRATs, at the time of writing. Thus, we can see that the birthrate problem (Keane & Kramer 2008) remains and RRATs must be explained within the context of known neutron star classes. Fortunately, this is possible.

### 5.1 When a Pulsar is a “RRAT”

We define a RRAT as:

**Definition:** A RRAT is a repeating radio source, with underlying periodicity, which is more significantly detectable via its single pulses than in periodicity searches.

This (arbitrary) definition is clearly a detection-based definition and a source can only be labelled a RRAT for a specific survey/telescope/observing frequency/observing time<sup>7</sup>. It says nothing directly about the intrinsic properties of the source — we feel that this is appropriate. Thus: *an observing setup might be contrived so as to make any pulsar a RRAT*. Are the group of RRATs, so defined, in any way

special? In a general sense, where any observational setup is possible, they are not, but for realistic survey specifications, they can be. Single-pulse searches make a selection on the parameter space of possible sources. The group of RRATs resulting from this may be of interest, for a number of reasons, as we will elucidate.

### 5.2 Selection Effects

We begin by considering what this definition means as far as selection effects are concerned. As an example, we can take a source, with period  $P$ , which emits (detectable) pulses a fraction of the time  $g$  and nulls (or is not detected) a fraction of the time  $1 - g$ . Then we can use the well-known selection effect in  $g - P$  space for this scenario (McLaughlin & Cordes 2003; Keane 2010a), namely  $r > 1$  when  $Tg^2/4 < P < Tg$ , where  $T$  is the observing time. For a given  $g$ , the low period limit defines the  $r = (S/N)_{\text{SP}}/(S/N)_{\text{FFT}} = 1$  condition, so that, at lower periods an FFT search is more effective. For higher periods than  $Tg$  there is unlikely to be even one pulse during the observation. Figure 7 shows a plot of  $g - P$  space with ‘RRAT-PSR’ boundaries marked for the 35-minute pointings of the PMPS. Here we are using our definition of ‘RRAT’, and using ‘pulsar/PSR’ as a synonym for ‘more easily, or only detectable in a periodicity search’. Thus PMPS RRATs are those sources in the light grey or white shaded regions. Different surveys will have different RRAT-PSR boundaries, e.g. the higher-latitude Parkes surveys analysed by BB10 had shorter pointings and hence different boundaries which are over-plotted on Figure 7. Thus

<sup>7</sup> In fact the RRAT label is not permanent: a source may be detected as a RRAT but subsequently be more easily detected in periodicity observations, even for identical observing setups. This was the case for the PMSingle source J1652–4406.

the ‘RRAT’ J1647–36 detected in the high-latitude surveys would have been detected as a ‘pulsar’ if it were surveyed in the PMPS. We note that, in reality, the  $g$  values we measure represent the *apparent* nulling fraction, i.e. the intrinsic values of  $g$  may be higher depending on the pulse-to-pulse modulation and distance to the source (Weltevrede et al. 2006; BB10). Periodicity searches also make a selection in  $g - P$  space, the dark grey region of Figure 7. In comparison to periodicity searches, single-pulse searches are sensitive to high period sources ( $\gtrsim 10$  s) with moderate nulling fraction ( $\sim 0.1$ ) down to very short period ( $\sim 10^{-3} - 10^{-1}$  s) sources with large nulling fraction ( $10^{-4} - 10^{-3}$ ).

From inspecting Figure 7, we can make a number of remarks. Firstly, we can see that the average ‘RRAT’ and ‘PSR’ periods we infer would be:

$$\langle P \rangle_{\text{RRAT}} = \frac{\int P(\int \text{RRAT}(g, P) dg) dP}{\int \int \text{RRAT}(g, P) dg dP}, \quad (4)$$

$$\langle P \rangle_{\text{PSR}} = \frac{\int P(\int \text{PSR}(g, P) dg) dP}{\int \int \text{PSR}(g, P) dg dP}, \quad (5)$$

where  $\text{RRAT}(g, P)$  and  $\text{PSR}(g, P)$  are distribution functions in  $g - P$  space. For a uniform  $g - P$  distribution these simply correspond to the shaded areas in the figure, and the results can be easily calculated. For sensible ranges (the ranges plotted in Figure 7, for  $P < 10$  s, say) we always get  $\langle P \rangle_{\text{RRAT}} > \langle P \rangle_{\text{PSR}}$ . It would not then be useful (or fair) to compare period distributions of sources selected in these ways. Further examining the figure we can see that the bottom left-hand corner (bounded by the black lines in the figure) is lacking in sources. Moving upwards a decade in  $P$  for the same  $g$  range (say) we expect to get  $\sim 10$  times as many sources, if the distribution is uniform, and this is, roughly, what we see. Going up another decade in  $P$  we do not see a further increase in sources, most likely due to there being no radio-visible pulsars with  $P \gtrsim 10$  s. The period distribution is approximately uniform in  $\log P$  in the band  $\sim 0.5 - 8$  s (given the small numbers of sources), which we contrast with the lognormal distribution for pulsars centred at 0.3 s (Ridley & Lorimer 2010).

The distribution in  $g$  may be of more interest. We can see that, within the band where we see sources, the distribution is not uniform, but looks somewhat uniform in  $\log g$ . We can thus explain the distribution of sources as follows: (i) The low  $P$ -low  $g$  region is devoid of sources as this does not represent a large area of parameter space and/or there are not many sources with these characteristics; (ii) The  $P \gtrsim 10$  s region does not have any active radio pulsars, consistent with what is expected for slow pulsars which have passed the death line; (iii) The  $P \sim 0.5 - 8$  s region for  $g \sim 10^{-4} - 10^{-1}$  shows a somewhat uniform distribution in  $\log g$ , suggesting that there are more RRAT-selected pulsars with high nulling fractions than would be expected from a uniform distribution in  $g - P$  space. To turn this around, if we search for RRATs, we are likely to find pulsars with high nulling fraction. These data are not sufficient to identify any trend in  $g$  with  $P$ , and there are less data for investigating any relationships with  $\dot{P}$ ,  $\tau$ ,  $B$ ,  $\dot{E}$ , etc. As a final comment on Figure 7 we note that there are several PMPS sources just above the light grey region. Here it is unlikely that there will be a pulse during a 35-minute pointing but nevertheless there are 8 sources. For each of these, which we were lucky to detect, we might expect there are several

similar sources, which we missed, simply due to probability. This is yet another argument, if any were needed, in favour of surveying the sky multiple times. Indeed the HTRU survey (Keith et al. 2010) is currently surveying the Galaxy at declinations  $\delta < 10^\circ$ , which includes the region covered by the PMPS, and has already identified new sources which were presumably ‘off’ during the 35-minute PMPS pointings (Burke-Spolaor et al. 2011b).

Slow-down rate,  $\dot{P}$ , is not subject to any selection effect in either RRAT or periodicity searches, as typical  $\dot{P}$  values have no effect during survey pointings. Looking at Figure 5 we can see that the  $\dot{P}$  values for 5 RRATs in particular are higher than average, with high corresponding magnetic field strengths of  $B \gtrsim 10^{13}$  G (less than 4% of the overall population have  $B$  values this high). Excluding J1554–5209 the other sources all have slightly higher than average magnetic fields with  $B > 10^{12}$  G, consistent with the earlier claim of McLaughlin et al. (2009). As single-pulse searches have no selection effects against high nulling fraction pulsars, and these same sources seem to have high- $B$  values, this suggests the question: Do long period and/or high- $B$  pulsars have higher nulling fraction? Here we reach a dead end as the nulling properties of pulsars are completely unknown in the  $B \sim B_{\text{QC}}$  and  $P \gtrsim 3$  s regions, where a number of RRATs are found. One reason for this is that these regions have a dearth of sources and in fact the PMPS RRATs represent a significant fraction of the known sources in these regions. As the PMPS RRATs are not obviously very distant we also ask the question: Do long period and/or high  $B$  pulsars have large modulation indices? Weltevrede et al. (2006, 2007) suggest a weak correlation of modulation index with  $B$ , but again, the number of high- $B$  and long period sources in this sample was small.

Another selection effect that the PMPS RRATs suffered from is the ‘low-DM blindness’ of the original single-pulse search, i.e. the possibility that low-DM sources were missed due to the effects of RFI. Our re-analysis removed this effect and in fact discovered a number of low-, as well as high-DM sources which had initially been missed due to RFI (see e.g. Figure 1 of K+10) so that we believe this selection effect has been largely removed.

### 5.3 Explanations of sporadic behaviour

There have been many ‘solutions’ proposed as to how a sporadic emission mechanism might operate, sometimes involving trigger mechanisms for (re-)activating pulsar emission due to transient disturbances in fall-back discs (Li 2006), surrounding asteroidal material (Cordes & Shannon 2008) or plasma trapped in radiation belts (Luo & Melrose 2007). However, as we have asserted that RRATs are merely pulsars which fit a particular selection criteria, for a given observational setup, the question of a solution becomes more a question of what types of pulsars are we most likely to detect as RRATs. There are two obvious types consistent with high observed nulling fractions: (i) weak/distant pulsars with high modulation indices; (ii) nulling pulsars. BB10 have dubbed “objects which emit only non-sequential single bursts with no otherwise detectable emission at the rotation period”, as ‘classic RRATs’, but by this definition, there may be no RRATs (see § 6.1) so we do not use this terminology.

The projected population of RRATs is not as high if

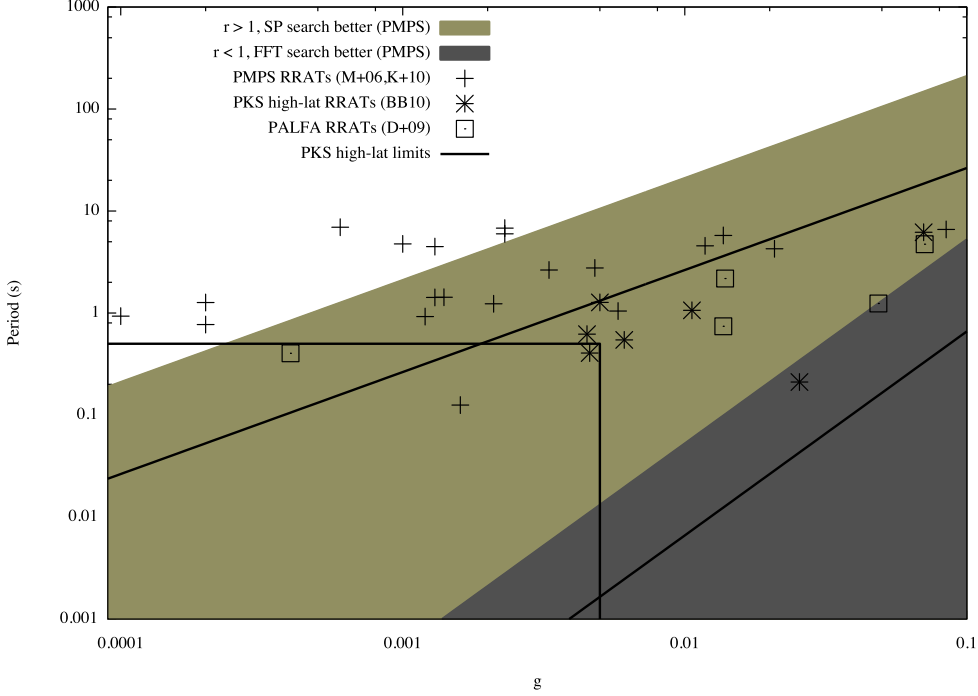


**Figure 7.** Plotted is  $g - P$  space, where  $g$  is the fraction of periods where a pulse is detected and  $P$  is the rotation period. Considering the ratio  $r = (S/N)_{\text{SP}} / (S/N)_{\text{FFT}}$  the regions where SP searches (light grey+white,  $r > 1$ ) and FFT searches (dark grey,  $r < 1$ ) are more effective for the PMPS are marked, defining “RRAT” and “pulsar” regions. Over-plotted are the PMPS RRATs with measured periods as reported in M+06 & K+10. Also plotted are the boundaries (black lines) for the sources reported by BB10 with known  $P$  and  $g$ . We also plot the sources reported in (Deneva et al. 2009) (D+09 in the figure). J1854+0306 is plotted with the PMPS sources, although it was also identified in PALFA. We note that the boundaries for the inner-Galaxy PALFA pointings are the same as for the Parkes high-latitude surveys if we assume no difference in sensitivity. This is of course incorrect, and due to this extra difference (the Parkes surveys have the same sensitivity as each other) the D+09 sources are plotted simply for illustration.

some sources are covered by solution (i). Such sources will have low-luminosity periodic emission. The pulsar population is estimated only above some threshold luminosity, typically  $L_{\min} \sim 0.1 \text{ mJy kpc}^2$ , so that if these sources are above  $L_{\min}$  they are already accounted for within low-luminosity selection-effect scaling factors in estimates of the pulsar population (Lorimer et al. 2006; Ridley & Lorimer 2010). If the underlying periodic emission were below  $L_{\min}$  then these sources would contribute to a birthrate problem by increasing the pulsar population estimate. In fact the required low-luminosity turn-over<sup>8</sup> is not yet seen, which is why artificial cut-offs are usually applied in population syntheses (see e.g. Faucher-Giguère & Kaspi (2006)). BB10 argue that extreme modulation can account for all but two RRATs, but notably not J1819–1458 and J1317–5759, which agrees with recent analysis by Miller et al. (2011, submitted). The true number covered by scenario (i) may be smaller as it assumes analogues of the extreme source PSR B0656+14 to be common in the Galaxy (BB10). So it appears that a number of RRATs are accounted for by scenario (i), whereas some are not, and seem to fit type (ii).

#### 5.4 Switching Magnetospheres?

Scenario (ii), which sees RRATs as nulling pulsars, extends the boundaries of observed nulling behaviour. In comparison to the previously observed nulling sample, RRATs would be considered extreme, with nulls of minutes to hours, as opposed to  $\sim$ seconds. Excluding the RRATs, nulling has been observed in  $\sim 50$  pulsars, but, if we include pulsars where an upper limit on the nulling fraction has been obtained, the number in the literature is  $\sim 100$  (Biggs 1992; Vivekanand 1995; Lorimer et al. 2002; Faulkner et al. 2004; Redman et al. 2005; Weltevrede et al. 2006; Wang et al. 2007). Of these, there are 50 with  $P > 1 \text{ s}$ , 10 with  $P > 2 \text{ s}$  and 1 with  $P > 3 \text{ s}$ . The nulling behaviour of long period and high-B sources is completely unknown. Some authors have claimed a correlation of nulling fraction with period (Biggs 1992), whereas others have claimed the correlation is instead with characteristic age (Wang et al. 2007). Some of the observed RRATs are high-B sources with long period, but are young in terms of characteristic age. Others are ‘dying’ pulsars having both long periods and old characteristic ages. Observations of a large sample of pulsars, selected as RRATs, could then be ideal for the purpose of testing these competing claims.

Thus, we have ‘nulling pulsars’, with nulls of 1 – 10 periods, ‘RRATs’ with nulls of 10 –  $10^4$  periods and ‘intermittent pulsars’ with nulls of  $10^4 - 10^7$  periods. It appears that there may be a continuum of null durations in the pulsar population. The question of the ‘RRAT emission mechanism’ is then subsumed by the questions of what makes pul-

<sup>8</sup> There must be a low-luminosity turn-over so that the integral  $\int N(L)dL$  does not diverge at the low end. Here  $N(L)dL$  denotes the number of pulsars with luminosity between  $L$  and  $L + dL$ .

sars null, and why such a wide range of null durations are possible. Another question of immediate interest is in what cases do nulls occur — high-B, long period, old pulsars? Also unexplained are the non-random (Redman & Rankin 2009) and periodic behaviour seen in several sources, e.g. 1-minute periodicity for PSR J1819+1305 (Rankin & Wright 2008), several minutes for the PMSingle source J1513–5946, hours for PSR B0826–34 (Durdin et al. 1979),  $\sim 1$  day for PSR B0823+26 (N. Young, private communication) and  $\sim 1$  month for PSR 1931+24 (Kramer et al. 2006). Considering the more general case of moding, we can add the pulsars reported by Lyne et al. (2010), which switch between (at least) 2 modes, with associated switches in spin-down rate. PSR J0941–39 is observed to switch between ‘RRAT-like’ and ‘pulsar-like’ modes (BB10). Recently PSR J1119–6127 has been observed to switch between RRAT, pulsar and null states (Weltevrede et al. 2010). Interestingly these changes, in the case of PSR J1119–6127, are seen to occur contemporaneously with the occurrence of an ‘anomalous glitch’, i.e. one resulting in a net decrease in spin-down rate, as seen only in RRAT J1819–1458 previously (Lyne et al. 2009).

The mounting evidence suggests that it is a general property of (at least some) pulsars, that they can switch back and forth between two stable states of emission. We note that, as  $\dot{E}_{\text{radio}} \ll \dot{E}$ , the simple switching on or off of the radio emission should not result in any noticeable effect<sup>9</sup> in  $\dot{\nu}$ . The fact that  $\dot{\nu}$  changes have been observed in very-long duration nullers (Kramer et al. 2006, the effect is unobservable in short-duration nullers) suggests a large-scale change in the magnetosphere, i.e. the nulls are not due to the micro-physics of the emission mechanism (Timokhin 2009). Within the framework of force-free magnetospheres, it has been shown that a number of stable solutions are possible with different sizes of the closed field line region (Contopoulos 2005; Timokhin 2006). These solutions are derived as for the original solution of Contopoulos et al. (1999), but without the assumption that the angular velocity of the field lines is equal to that of the star. Timokhin (2009) has shown how moderate changes in the beam shape and/or current density can cause large changes in  $\dot{E}$ , and hence  $\dot{\nu}$ . For a pulsar changing between two stable states, the observed emission along our line of sight will change, and this will be seen as a mode switch. A null will result if the beam moves out of our line of sight as a result of the switch, or, if there is a sufficient change in current such that the emission ceases (Timokhin 2009). Contopoulos (2005) have shown that a sudden depletion of charges will result in such a change of state (which they refer to as a ‘coughing magnetosphere’), but with no explanation for why this depletion might arise. A recent suggestion by Rosen et al. (2011) is that the required change in charge density might be triggered by non-radial oscillations of the stellar surface, although no driving mechanism for such oscillations is yet known. What is clear from the data is that pulsars can switch between stable states. Such an effect, if

truly a generic property of pulsars, can explain the phenomena of moding, nulling and RRATs. The theoretical work shows that different stable magnetospheric states exist. The reason why a pulsar would switch between two states (in particular with a periodicity) is unknown.

## 6 CONCLUSION

### 6.1 Facts about RRATs

We now address a number of assertions, claims and misconceptions concerning the characteristics of RRATs, that we have encountered during the last few years. Firstly, the assumption that all RRATs have high magnetic field strengths is incorrect. If we arbitrarily define high-B as  $B \geq 10^{13}$  G, then there are 5 (or 4) RRATs in this category using minimum  $B$  values for the vacuum (or force-free) case. Neither is it true that RRATs and magnetars are linked in some way, despite the tentative link suggested for J1819–1458 due to its unusual glitches. Although true of the data accumulated up to the original discovery paper of M+06, it is no longer a true statement to say that RRATs are only detectable in single-pulse searches. Several of the original, PMSingle and BB10 sources are detectable in periodicity searches, in some cases occasionally and in some cases reliably. Similarly the pulse arrival times do not seem to be random. We have discussed non-random behaviour (here, and in K+10) in the PMSingle sources, where clustering of pulses is seen, e.g. in J1724–35 and J1513–5946. This is also seen in J1913+1330 at Jodrell Bank and at Parkes (McLaughlin 2009; Keane 2010a). Consecutive pulses from RRATs are seen quite often. We detect consecutive pulses in several PMSingle sources, and in our ongoing observations of J1819–1458 and J1913+1330 at Jodrell Bank, and Palliyaguru et al. (2011, submitted) report higher instances of doublets, triplets and quadruplets than would be expected by random chance. Palliyaguru et al. also report an instance of detecting pulses from J1819–1458 for 9 consecutive periods. This drastically changes the ‘activation timescales’ needed in some models (although not all, see e.g. Zhang et al. (2007)) of RRAT emission, from  $\sim 3$  ms to  $\sim 35$  s. We can also say that none of the RRATs discovered, which have coherent timing solutions, are in binary systems.

### 6.2 Questions & Future Work

Our studies of RRATs raise a number of questions and suggest a number of lines of enquiry for future work. For instance, we do not know the significance of the anomalous glitches seen in both J1819–1458 and J1119–6127, both pulsars lie in the  $B \sim B_{\text{QC}}$  region of  $P - \dot{P}$  space, although there is evidence linking these glitches with changes in radio emission behaviour (Weltevrede et al. 2010). It would seem that an investigation of all sources (and indeed searches for more) in this region is warranted. With the discoveries of neutron stars which switch between 2 or more stable states, it is timely, and necessary, to perform a complete census of nulling pulsars across the  $P - \dot{P}$  diagram, as nulling properties are known for only a relatively small fraction of the pulsar population, and are unknown for high-B and long-period sources. The cause of nulling is unknown:

<sup>9</sup> Consider a simple calculation for a pulsar with radio flux density of 10 mJy, a distance 1 kpc away. Its radio pseudoluminosity is then  $10^{-2} \text{ Jy kpc}^2 \approx 10^{11} \text{ W Hz}^{-1}$ . Assuming a constant flux density over a GHz bandwidth gives a luminosity of  $E_{\text{radio}} = 10^{20} \text{ J.s}^{-1} = 10^{27} \text{ erg s}^{-1}$  which we can compare to the much higher  $\dot{E}$  values reported in Table 1.

does slowing down below a critical rotation rate, or a magnetic field growing/decaying to a certain value, signal the onset of nulling?

It is unknown what decides whether neutron stars with similar spin properties will manifest themselves as RRATs, as opposed to (say) a magnetar or an XDINS. The answer to this important question is fundamental if there is to be “grand unification of neutron stars” (Kaspi 2010), i.e. the determination of some kind of evolutionary framework. For example, the region of  $P - \dot{P}$  space defined by  $P = 4-10$  s,  $\dot{P} = 10^{-13}-10^{-12}$  contains radio pulsars (some ‘normal’ pulsars, some RRATs like J1819–1458), magnetars and XDINSs. For very similar spin-down properties we have very different observational manifestations. We might speculate that these different classes, although having similar properties now, have evolved in completely different ways and may have completely different ages. The snapshot we see now where these sources seem similar, may then be misrepresentative of their overall evolutionary behaviour. Alternatively, the conditions for coherent radio emission may be very sensitive, with this region a particular area of parameter space on the threshold for emission. This is perhaps consistent with the transient radio emission seen in magnetars and the extreme nulling of the RRATs in this region. If the re-connection rate at the Y-point (separating open and closed field lines in the magnetosphere, see e.g. Spitkovsky (2006)) were slow, or progressed in steps, then bursts of radio emission may be expected between dormant phases, when the magnetospheric configuration was favourable. A natural explanation for periodic switching between stable magnetospheric states is still lacking.

The many transient searches underway highlight more basic questions also, such as what can we use as a reliable estimate of age for neutron stars (important if an evolutionary framework is ever to exist), how many neutron stars are there in the Galaxy, and how many sources remain to be discovered in the archives of existing pulsar surveys as yet undiscovered. What we do know is that those pulsars discovered as RRATs are now beginning to represent a significant number, yet there does not seem to be real cause for concern regarding the expected number of such sources being discovered. The emission seen in RRATs does not seem remarkable, other than in its sporadicity, so that there is no need to formulate any new emission mechanisms. They can be explained within the existing pulsar framework, or rather, the existing framework of open questions. Interestingly, with single-pulse searches, we have a means with which to identify pulsars which have been difficult to find, in particular the high-B and the dying pulsars.

## ACKNOWLEDGMENTS

EK acknowledges the FSM, the support of a Marie-Curie EST Fellowship with the FP6 Network “ESTRELA” under contract number MEST-CT-2005-19669, STFC RG R108020 and helpful discussions about pulsar timing with Mark Purver & Kuo Liu. MAM is an Alfred P. Sloan Fellow and is supported by the Research Corporation. The Parkes radio telescope is part of the Australia Telescope National Facility which is funded by the Commonwealth of Australia for operation as a National Facility managed by CSIRO.

## REFERENCES

- Backer D. C., 1970, *Nature*, 228, 42
- Baring M. G., Harding A. K., 1998, *ApJ*, 507, L55
- Bartel N., Morris D., Sieber W., Hankins T. H., 1982, *ApJ*, 258, 776
- Bastian T. S., 1994, *Space Science Reviews*, 68, 261
- Bhat N. D. R., Cordes J. M., Camilo F., Nice D. J., Lorimer D. R., 2004, *ApJ*, 605, 759
- Biggs J. D., 1992, *ApJ*, 394, 574
- Boyles J. et al., 2010, in *Bulletin of the American Astronomical Society*, Vol. 41, BAAS, p. 464
- Burke-Spolaor S., Bailes M., 2010, *MNRAS*, 402, 855
- Burke-Spolaor S., Bailes M., Ekers R., Macquart J., Crawford F., III, 2011a, *ApJ*, 727, 18
- Burke-Spolaor S. et al., 2011b, *MNRAS*, in press
- Chen K., Ruderman M., 1993, *ApJ*, 402, 264
- Cognard I., Shrauner J. A., Taylor J. H., Thorsett S. E., 1996, *ApJ*, 457, L81
- Contopoulos I., 2005, *A&A*, 442, 579
- Contopoulos I., Kazanas D., Fendt C., 1999, *ApJ*, 511, 351
- Cordes J. M., Lazio T. J. W., preprint (arXiv:astro-ph/0207156)
- Cordes J. M., Lazio T. J. W., McLaughlin M. A., 2004, *New Astronomy Review*, 48, 1459
- Cordes J. M., Shannon R. M., 2008, *ApJ*, 682, 1152 (astro-ph/0605145)
- Cordes J. M., Shannon R. M., 2010, *ArXiv e-prints*
- Deller A. T., Tingay S. J., Bailes M., Reynolds J. E., 2009, *ApJ*, 701, 1243
- Deneva J. S. et al., 2009, *ApJ*, 703, 2259
- Dhillion V. S. et al., 2011, *MNRAS*, in press
- Dulk G. A., 1985, *Ann. Rev. Astr. Ap.*, 23, 169
- Durbin J. M., Large M. I., Little A. G., Manchester R. N., Lyne A. G., Taylor J. H., 1979, *MNRAS*, 186, 39P
- Eatough R. P., Keane E. F., Lyne A. G., 2009, *MNRAS*, 395, 410
- Edwards R. T., Bailes M., van Straten W., Britton M. C., 2001, *MNRAS*, 326, 358
- Edwards R. T., Hobbs G. B., Manchester R. N., 2006, *MNRAS*, 372, 1549
- Espinoza C. M., 2009, Ph.D. thesis, University of Manchester
- Espinoza C. M., Lyne A. G., Stappers B. W., Kramer M., 2011, *MNRAS*, in press
- Faucher-Giguère C.-A., Kaspi V. M., 2006, *ApJ*, 643, 332
- Faulkner A. J. et al., 2004, *MNRAS*, 355, 147
- Hansen B. M. S., Lyutikov M., 2001, *MNRAS*, 322, 695
- Helfand D. J., Manchester R. N., Taylor J. H., 1975, *ApJ*, 198, 661
- Hessels J. W. T., Ransom S. M., Kaspi V. M., Roberts M. S. E., Champion D. J., Stappers B. W., 2008, in *American Institute of Physics Conference Series*, Vol. 983, C. Bassa, Z. Wang, A. Cumming, & V. M. Kaspi, ed, 40 Years of Pulsars: Millisecond Pulsars, Magnetars and More, p. 613
- Hobbs G., Manchester R., Teoh A., Hobbs M., 2004, in *Young Neutron Stars and Their Environments*, Vol. 1, Camilo F., Gaensler B. M., ed, IAU Symposium 218. Astronomical Society of the Pacific, San Francisco, p. 139
- Hobbs G. B., Edwards R. T., Manchester R. N., 2006, *MNRAS*, 369, 655



- Hyman S. D., Lazio T. J. W., Roy S., Ray P. S., Kassim N. E., 2006, *ApJ*, 639, 348
- Ioka K., 2003, *ApJ*, 598, L79
- Jacoby B. A., Bailes M., Ord S. M., Edwards R. T., Kulkarni S. R., 2009, *ApJ*, 699, 2009
- Karuppusamy R., Stappers B. W., van Straten W., 2010, *MNRAS*, 401, A36
- Kaspi V. M., 2010, *ArXiv e-prints* (astro-ph/1005.0876)
- Keane E. F., 2010a, Ph.D. thesis, University of Manchester
- Keane E. F., 2010b, *ArXiv e-prints* (astro-ph/1008.3693)
- Keane E. F., Kramer M., 2008, *MNRAS*, 391, 2009
- Keane E. F., Ludovici D. A., Eatough R. P., Kramer M., Lyne A. G., McLaughlin M. A., Stappers B. W., 2010, *MNRAS*, 401, 1057
- Keith M. J. et al., 2010, *MNRAS*, 409, 619
- Kramer M., Lyne A. G., O'Brien J. T., Jordan C. A., Lorimer D. R., 2006, *Science*, 312, 549
- Li X.-D., 2006, *ApJ*, 646, L139
- Lorimer D. R., Bailes M., McLaughlin M. A., Narkevic D. J., Crawford F., 2007, *Science*, 318, 777
- Lorimer D. R., Camilo F., Xilouris K. M., 2002, *ApJ*, 123, 1750
- Lorimer D. R. et al., 2006, *MNRAS*, 372, 777
- Lorimer D. R., Kramer M., 2005, *Handbook of Pulsar Astronomy*. Cambridge University Press
- Luo Q., Melrose D., 2007, *MNRAS*, 378, 1481
- Lyne A., Hobbs G., Kramer M., Stairs I., Stappers B., 2010, *Science*, 329, 408
- Lyne A. G., Manchester R. N., 1988, *MNRAS*, 234, 477
- Lyne A. G., McLaughlin M. A., Keane E. F., Kramer M., Espinoza C. M., Stappers B. W., Palliyaguru N. T., Miller J., 2009, *MNRAS*, 400, 1439
- Lyne A. G., Smith F. G., 2004, *Pulsar Astronomy*, 3rd ed. Cambridge University Press, Cambridge
- Manchester R. N. et al., 2001, *MNRAS*, 328, 17
- McLaughlin M., 2009, in *Astrophysics and Space Science Library*, Vol. 357, W. Becker, ed, *ASSL*, p. 41
- McLaughlin M. A., Cordes J. M., 2003, *ApJ*, 596, 982
- McLaughlin M. A. et al., 2009, *MNRAS*, 400, 1431
- McLaughlin M. A. et al., 2006, *Nature*, 439, 817
- McLaughlin M. A. et al., 2007, *ApJ*, 670, 1307
- Osten R. A., 2008, *ArXiv e-prints* (astro-ph/0801.2573)
- Osten R. A., Bastian T. S., 2008, *ApJ*, 674, 1078
- Phinney S., Taylor J. H., 1979, *Nature*, 277, 117
- Rankin J. M., 1993, *ApJ*, 405, 285
- Rankin J. M., Wright G. A. E., 2008, *MNRAS*, 385, 1923
- Rathnasree N., Rankin J. M., 1995, *ApJ*, 452, 814
- Rea N. et al., 2009, *ApJ*, 703, L41
- Redhead A. C. S., 1994, *ApJ*, 426, 51
- Redman S. L., Rankin J. M., 2009, *MNRAS*, 395, 1529
- Redman S. L., Wright G. A. E., Rankin J. M., 2005, *MNRAS*, 357, 859
- Rees M. J., 1977, *Nature*, 266, 333
- Reynolds S. et al., 2006, *ApJ*, 639, L71
- Richards M. T., Waltman E. B., Ghigo F. D., Richards D. S. P., 2003, *ApJS*, 147, 337
- Ridley J. P., Lorimer D. R., 2010, *MNRAS*, 404, 1081
- Romani R., Johnston S., 2001, *ApJ*, 557, L93
- Rosen R., McLaughlin M. A., Thompson S. E., 2011, *ApJ*, 728, L19
- Rubio-Herrera E., 2010, Ph.D. thesis, University of Amsterdam
- Shapiro S. L., Teukolsky S. A., 1983, *Black Holes, White Dwarfs and Neutron Stars. The Physics of Compact Objects*. Wiley-Interscience, New York
- Shitov Y. P., Kuzmin A. D., Dumskii D. V., Losovsky B. Y., 2009, *Astronomy Reports*, 53, 561
- Spitkovsky A., 2006, *ApJ*, 648, L51
- Taylor J. H., 1990, in Backer D. C., ed, *Impact of Pulsar Timing on Relativity and Cosmology*. Center for Particle Astrophysics, Berkeley, p. m1
- Timokhin A. N., 2006, *MNRAS*, 368, 1055
- Timokhin A. N., 2009, *ArXiv e-prints* (astro-ph/0912.2995)
- Vivekanand M., 1995, *MNRAS*, 274, 785
- Vranešević N., Melrose D. B., 2010, *MNRAS*, 1768
- Wang N., Manchester R. N., Johnston S., 2007, *MNRAS*, 377, 1383
- Weltevredre P., Edwards R. T., Stappers B. W., 2006, *A&A*, 445, 243
- Weltevredre P., Johnston S., Espinoza C. M., 2010, *ArXiv e-prints*
- Weltevredre P., Stappers B. W., Edwards R. T., 2006, *A&A*, 469, 607
- Weltevredre P., Stappers B. W., Rankin J. M., Wright G. A. E., 2006, *ApJ*, 645, L149
- Zarka P., 1998, *Journal of Geophysical Research*, 20, 159
- Zhang B., J. G., J. D., 2007, *MNRAS*, 374, 1103